<u>CHAPTER 4</u> ACCURACY OF THE IMPROVED TWO GENERATOR MODEL SWING LOCUS

This dissertation uses the improved two generator model to show that shunts affect the impedance locus the swing traces and shows that the accuracy with which the classical two generator model traces the actual swing locus greatly improves when the network shunts are included.

The network model obtained when the classical two generator model includes the shunts is referred to using the phrase “improved two generator model”.

Most texts use a simple network model, i.e. classical model, with simple network dynamics [1], [13], [23] and [45]. The network dynamics are kept simple by keeping the network impedance constant and by using the constant voltage behind transient reactance generator model. The simple network model does not include shunts.

Therefore, to make the results obtained with the improved two generator model comparable with the texts on out-of-step relaying, the improved two generator model uses the constant voltage behind transient reactance generator model and the external network impedance is kept constant.

To show that the improved two generator model does not over- or under emphasise the affect shunts have, the locus the improved two generator model traces is compared with the locus the detailed network model traces. The improved two generator model uses a constant impedance load model. Therefore, the detailed network model uses a constant impedance load model.

The above comparison assumes that the swing locus the detailed network model traces is realistic. Section 4.1 discusses the factors that are considered to ensure that the detailed network model traces a realistic swing locus.

The view of texts on out-of-step relaying is that simple network models should only be used to understand the results obtained with more complex networks (Chapter 2, section 2.5.1). To show that this is the case for the improved two generator model, the impedance locus the improved two generator model traces is compared with the impedance locus the detailed network model traces when the load includes large and small induction motors.

4.1 ENSURING THE SWING LOCUS IS REALISTIC

The impedance locus the swing traces can be obtained by computing the seen impedance, $\boldsymbol{Z_C}$, for the angles $\delta \in \left[0^\circ ;360^\circ\right]$.

The reactances and internal voltages of the generators slipping poles, the impedances of the lines that make up the network and the impedances of the network shunts determine the numerical value of $\boldsymbol{Z_C}$ (Chapter 2, section 2.5.1).

Therefore, the swing locus the detailed network model traces will be realistic when the generators, external network and network protection operation are modelled accurately.

This section discusses the modelling the detailed network model uses and discusses the factors the detailed network model considers to ensure that the generators, external network and network protection operation are modelled accurately.

4.1.1 Modelling the generators

The principal factors affecting the dynamic behaviour of the generators in the perturbation bandwidth DC to about 10 Hz are the rotor flux linkage transients and the possible saturation of the magnetic circuit.

These factors are covered by PSS/E. Specifically the PSS/E GENROU generator model correctly represents the generator electromagnetic, synchronising and damping effects over the bandwidth DC to 10 Hz.

The slip frequency expected when Mpumalanga and the Western Cape are slipping poles is of the order of 1.72 Hz (figure 4.8). Consequently, the bandwidth DC to 10 Hz is adequate for the network disturbance this dissertation considers.

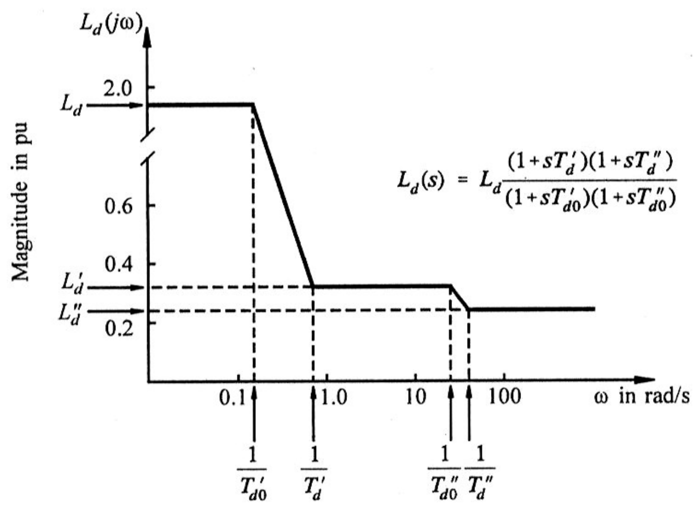

FIGURE 4.1 Sample variation of the magnitude of $L_d(s)$ [1, p160]

Model GENROU models the generator reactances up to the subtransient level – the variation, as a function of frequency, of the magnitude of the d-axis operational inductance, $L_d(s)$, is modelled as is shown in figure 4.1. The frequency plot is based on equation 4.1-a.

The similarities between equations 4.1-a and 4.1-b imply that the behaviour of $L_q(s)$ and $L_d(s)$ as a function of frequency are similar.

$L_d(s)$ and $L_q(s)$ can be computed using:

$$L_d(s) = L_d \frac{(1+sT_d^{'})(1+sT_d^{''})}{(1+sT_{d0}^{'})(1+sT_{d0}^{''})} \tag{4.1-a}$$

$$L_q(s) = L_q \frac{(1+sT_q^{'})(1+sT_q^{''})}{(1+sT_{q0}^{'})(1+sT_{q0}^{''})} \tag{4.1-b}$$

The data required by the above equations are obtained from the Eskom Dynamic Database.

In the representation of magnetic saturation for stability studies it is assumed only the mutual inductances, L_{ad} and L_{aq}, saturate.

The open-circuit saturation curve is used to represent the saturation characteristic.

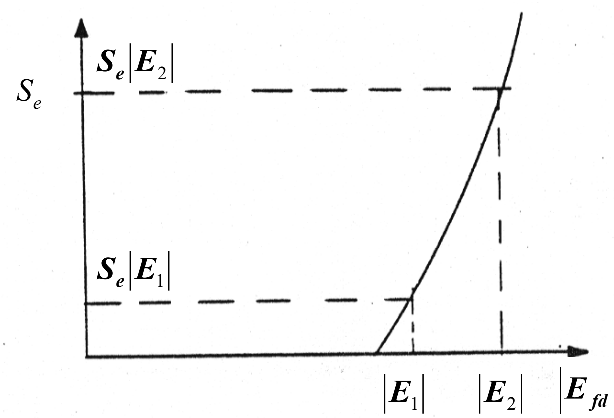

FIGURE 4.2 Defining the saturation function S_E [42, p15-4]

Model GENROU assumes that the saturation curve is quadratic and passes through the two points defined in figure 4.2. The saturation function, S_e, can be computed using [42, p15-1]:

$$S_e = \frac{B\left(E_{fd} - A\right)^2}{E_{fd}} \tag{4.2}$$

The saturation function S_e is a design characteristic of the exciter.

The exciter models available in PSS/E assume S_e can be calculated using equation 4.2.

Excitation systems affect the damping and synchronising torques. To be sure both these torques are accurately modelled, the parameters of the excitation systems of the detailed network model are obtained from the Eskom database.

The initial value of the voltage, $\boldsymbol{E}'$, behind transient reactance will be correct when the steady state operating point of the generator is correct (Appendix F).

4.1.2 Modelling the external network

The external network links the generation pools slipping poles and is made up of transmission lines and shunts. The shunts include loads and voltage regulating devices.

4.1.2.1 Load model used

The impedance locus the detailed network model traces is used to determine if the improved two generator model traces a real impedance locus. The procedure used is to compare the former and latter swing loci.

For the case where the comparison is done to determine if the improved two generator model can be used to illustrate the affect network shunts have on the swing locus the load situated in the detailed network model is changed to constant impedance.

For the case where the comparison is done to determine if the improved two generator model can be used to obtain the settings applied to out-of-step relays, the load situated in the detailed network model is changed to a composite load – i.e. load includes induction motors, discharge lighting, etc.

To explain why the composite load model is used, we note load models are classified into two broad categories: static models and dynamic models.

Static load models are applicable when the response of the load to voltage and frequency changes is fast and the steady state of the response is reached very quickly. This is true of most amplitudes of voltage and/or frequency change that are fairly small [1, p274].

Hence, the parameters of the static load model are based on the voltage and frequency dependency of the load observed within a limited range of voltage and frequency variations. The range of voltage variations static load models are valid for is normally $\pm 10\%$ [34, p74]; [49, p2-2].

The possible range of frequency variations is limited – often less than ± 3 Hz, i.e. ± 6 %, even for cases like islanding. The possible range of voltage variations is wide – e.g. 0% to 120% [51, p970].

Dynamic load models should be used when the excursion in frequency and voltage is large. The reason is the dynamics of the load components become important.

The study of interarea oscillations, voltage stability and long-term stability often require the modelling of the load dynamics. The study of networks with large concentration of motors also requires representation of load dynamics [1, p274].

When slipping poles, busbars close to the electrical centre experience large excursions in voltage. Hence, the load at these busbars should be modelled using the dynamic load model.

The chance of numerical instability occurring increases when the number of dynamic models used increases. To avoid numerical instability, static models are used to model the load situated far from the electrical centre.

4.1.2.1.1 Static load model used

The busbar voltage at Tutuka, Atlas and Grootvlei remains approximately at the steady state value during the first slip cycle (Chapter 3, figure 3.6). Hence, the load north of Tutuka, Atlas and Grootvlei can be modelled using the static load model. The static model used is the ZIP load model.

The ZIP model is made up of constant impedance, constant current and constant power components. The parameters of the model are the coefficients p_1 to p_3 and q_1 to q_3. These parameters define the proportion of each component.

The ZIP model computes the response of the load using [1, p272]:

$$P = P_0\left[p_1\overline{V}^2 + p_2\overline{V} + p_3\right]$$

$$Q = Q_0\left[q_1\overline{V}^2 + q_2\overline{V} + q_3\right] \tag{4.3}$$

$$\overline{V} = \frac{V}{V_0}$$

P and Q are the active and reactive components of the load when the voltage magnitude is V. The subscript 0 identifies the numerical values of the respective variables at the initial operating point.

In the absence of specific information, the most commonly accepted static load model is to represent active power as constant current (i.e. $p_1 = p_3 = 0$; $p_2 = 1$) and reactive power as constant impedance (i.e. $q_2 = q_3 = 0$; $q_1 = 1$) [1, p273].

The detailed network model uses $p_1 = p_3 = 0$, $p_2 = 1$ and $q_2 = q_3 = 0$, $q_1 = 1$.

4.1.2.2 Dynamic load model used

The excursion in voltage experienced at most of the busbars south of Tutuka, Atlas and Grootvlei exceeds 10% (figure 4.3). Hence, the static load model should not be used at busbars situated south of Tutuka, Atlas and Grootvlei.

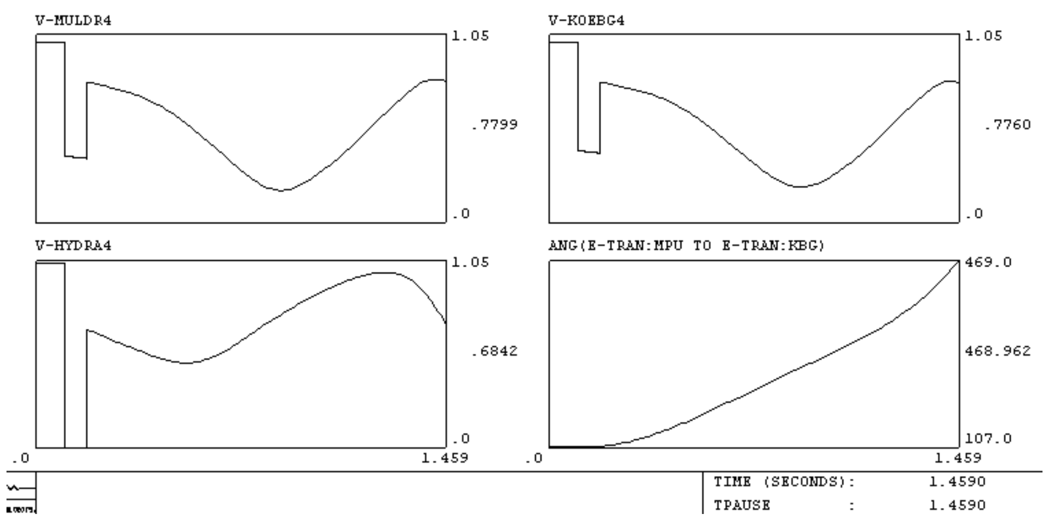

FIGURE 4.3 The voltage at the Koeberg, Muldersvlei and Hydra busbars during the first slip cycle

To identify the load model that should be used to model the load south of Tutuka, Atlas and Grootvlei, we note: "First swing cases exhibit large and rapid voltage excursions during the initiating fault and slower voltage excursions during the first power angle swing, which lasts approximately one second or less. Load response to these voltages is important. There is also a brief frequency excursion during the slip cycle. Hence, the frequency characteristics of the load close to the accelerating or decelerating generators could be important" [50, p476] and "…to ensure accuracy, stability studies should use load models that include the effect of motor inertia, motor rotor flux transients, contactor drop-out, discharge lighting discontinuities, etc." [50, p479].

The load model CLOAD includes most of the above requirements. CLOAD is available in PSS/E.

To clarify, we note CLOAD includes dynamic models of aggregations of large and small motors, non-linear model of discharge lighting, transformer saturation effects, constant MVA load, shunt capacitor, static load characteristics and a series impedance and tap ratio to represent the effect of intervening sub-transmission and distribution elements.

Figure 4.4 shows the make up of CLOAD.

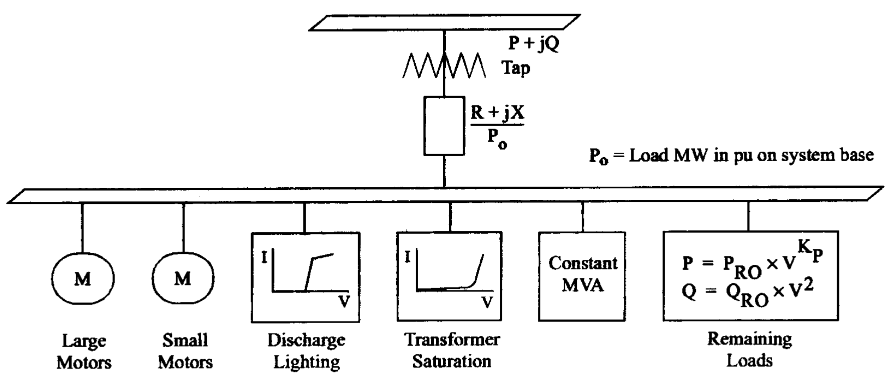

FIGURE 4.4 Composite load model PSS/E uses [46, pJ-20]

This dissertation uses model CLOAD to model the load south of Tutuka, Atlas and Grootvlei.

The characteristics of the induction motors, discharge lighting and transformer excitation are hard coded into the CLOAD model.

Table 4.1 Induction motor parameters CLOAD uses [48, p2]

PARAMETER	SMALL MOTOR	LARGE MOTOR
Rated slip	0.0294	0.0097
Full load torque	0.794	0.871
Full load power factor	0.832	0.886
Slip at maximum torque	0.15	0.06
Maximum torque	1.91	2.52
I_{LR}	4.8	6.55
T_{LR}	0.883	1.55
PF_{LR}	0.376	0.334
No load current (I_{NL})	0.43	0.325
H (including load)	0.5	1.0
D ($T_{LOAD} \approx (1-s)^D$)	1.0	1.0

The induction motor parameters CLOAD uses are listed in table 4.1. The induction motor model is fully frequency dependent and includes saturation in the exciting branch of the equivalent circuit. The rotor flux time constants are neglected.

With regard to induction motors, we note motor load makes up a large portion (50% 60%) of the total load [50, p478]. Hence, motors account for the major dynamic effects during certain disturbances [49, p2-16].

EPRI defines small motors to be 5 hp up to 200 hp motors ($H = 0.7$) and defines large motors to be 200 hp and up ($H = 1.5$) [49, p7-71].

The dynamic behaviour of large induction motors should be modelled using a detailed induction motor model. For smaller motors a simpler model involving the steady state equivalent circuit and the inertial differential equation is often adequate [34, p76]. Stator flux dynamics are normally neglected in stability analysis and the rotor flux dynamics may sometimes be neglected, particularly for long-term dynamic analysis [50, p474].

CLOAD, models discharge lighting (i.e. mercury vapour, sodium vapour and fluorescent lighting) to have an initial power factor of 0.93. The real part is constant current down to 75 percent voltage. The current then decreases linearly to zero as the voltage falls from 75 percent to 65 percent. The imaginary component of discharge lighting varies with voltage to the 4.5 exponent [48, p2].

This dissertation sets the transformer exciting current to 2%. To explain the effect transformer exciting current has, we note if normal voltage is applied to the primary terminals of a transformer with the secondary open circuited, a small excitation current flows. This current is made up of the magnetising and loss components. The economic design of a transformer dictates working the iron at the curved part of the saturation curve resulting in appreciable saturation at normal voltage. Hence, any increase in terminal voltage above normal will greatly increase the exciting current – e.g. a 108 percent terminal voltage could result in a 200 percent exciting current. Transformer exciting current can vary from 2% up to 4% [47, p413]. Exciting current varies directly with the voltage and inversely with the KVA rating.

CLOAD models transformer exciting current as a reactive load [48, p2].

The voltage excursions experienced in the section of the network where the load is modelled using CLOAD is large (figure 4.3). This allows the constant power portion of CLOAD to be set zero. To clarify, we note switch mode and other regulated power supplies make electronic devices such as computers, microwave ovens, TV's, etc. have a constant power characteristic down to 0.9 p.u. voltage.

Below 0.9 p.u. these loads cease to function [50, p478]. Adjustable speed drives behave like the aforementioned electronic devices, except shutdown will occur when the voltage drops below the lowest tolerance – approximately 0.9 p.u. [50, p478].

With regard to the “remaining load” component of CLOAD, we note this dissertation lumps all essential static load, e.g. resistive and incandescent lighting load [50, p473] under the “remaining load” component. The real component of the “remaining load” is set to vary as the voltage to the power $K_P = 2$. Appendix G identifies which percentage of the network is essential static load.

CLOAD automatically taps the transformers of the intervening sub-transmission and distribution networks. The tapping is done to ensure the desired initial load voltage is achieved. The impedance of a distribution transformer, on transformer MVA base, is between 8% and 12% [34, p69]. This dissertation stets the reactance of the mentioned transformers to 0.1 p.u. on transformer base MVA.

CLOAD includes a shunt capacitor bank. The capacitor bank is automatically sized to supply the reactive requirements of the motor, discharge lighting, transformer excitation and any sub-transmission and /or distribution impedance not supplied by the Main Transmission Network. The reactive component of the “remaining load” is lumped with the shunt capacitor – i.e. varies as the voltage raised to the 2^{nd} power.

Table 4.2 Load components of CLOAD

DESCRIPTION	PERCENTAGE OF BUSBAR LAOD [%]
Large motor	8.9
Small motor	53.6
Discharge lighting	12.2
Constant power	0
Remaining load	25.3

Table 4.2 lists the percentage load assigned to each load component CLOAD models. The percentages listed are obtained from Appendix G.

Table 4.3 lists the values used for exciting current, K_P, transformer resistance and transformer reactance.

Table 4.3 Parameters CLOAD uses

DESCRIPTION	VALUE
Transformer exciting current	2%
K_P of remaining load	2
Transformer resistance (p.u. on load MVA base)	0.0001
Transformer reactance (p.u. on load MVA base)	0.1

4.1.2.3 Static Var Compensators

Static Var Compensators (SVCs) are shunt connected VAR generators or absorbers whose outputs are varied in order to control specific parameters of the electric network.

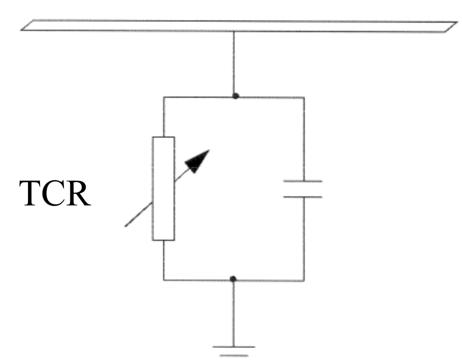

FIGURE 4.5 Controlled reactor and fixed capacitor to provide controlled VAR supply

The SVCs installed in the tie line linking Mpumalanga to the Western Cape controls the negative phase sequence voltage to ensure a minimum phase unbalance. This mode of control is sustained until any of the SVC's three phases reaches its reactive or capacitive limit or the positive phase sequence voltage at the SVC high voltage busbar is no longer within the 1.05 p.u. to 0.95 p.u. band of allowed voltages. The SVC then switches to controlling the positive phase sequence voltage. PSS/E models only the control of the positive phase sequence voltage.

The steady state operating point of the SVC is determined by the SVC droop. PSS/E uses the reactance of the main SVC transformer to represent the droop. The droop settings are obtained from the Eskom Dynamic Database.

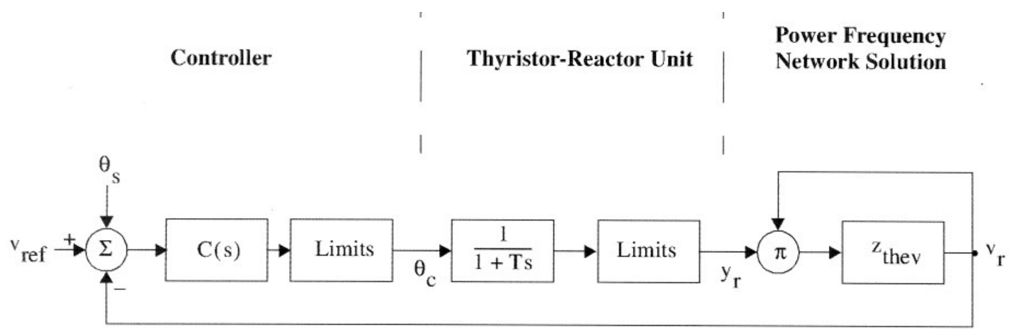

FIGURE 4.6 Form of Static VAR System representation PSS/E uses [42, p14-4]

The Thyristor-Controlled-Reactor or TCR (figure 4.5) is the only SVC element with a variable output. The response time of the TCR is typically 1 to 5 cycles of the supply frequency – i.e. 20 to 100 milliseconds.

The detailed network model uses model CSVGN1 to control the firing of the thyristors of the TCR.

The parameters shown in figure 4.6 have the following meanings: v_r is the bus voltage; i_r is the controlled reactor current; y_r is the effective controlled reactor admittance; θ_c is the reference signal for thyristor firing control; θ_s is the supplementary signal and v_{ref} is the reference voltage.

The parameters model CSVGN1 uses are obtained from the Eskom Dynamic Database.

Figure 4.7 shows when slipping poles the Hydra SVCs of the detailed model moves from zero VAR support to full absorbing within 200 milliseconds.

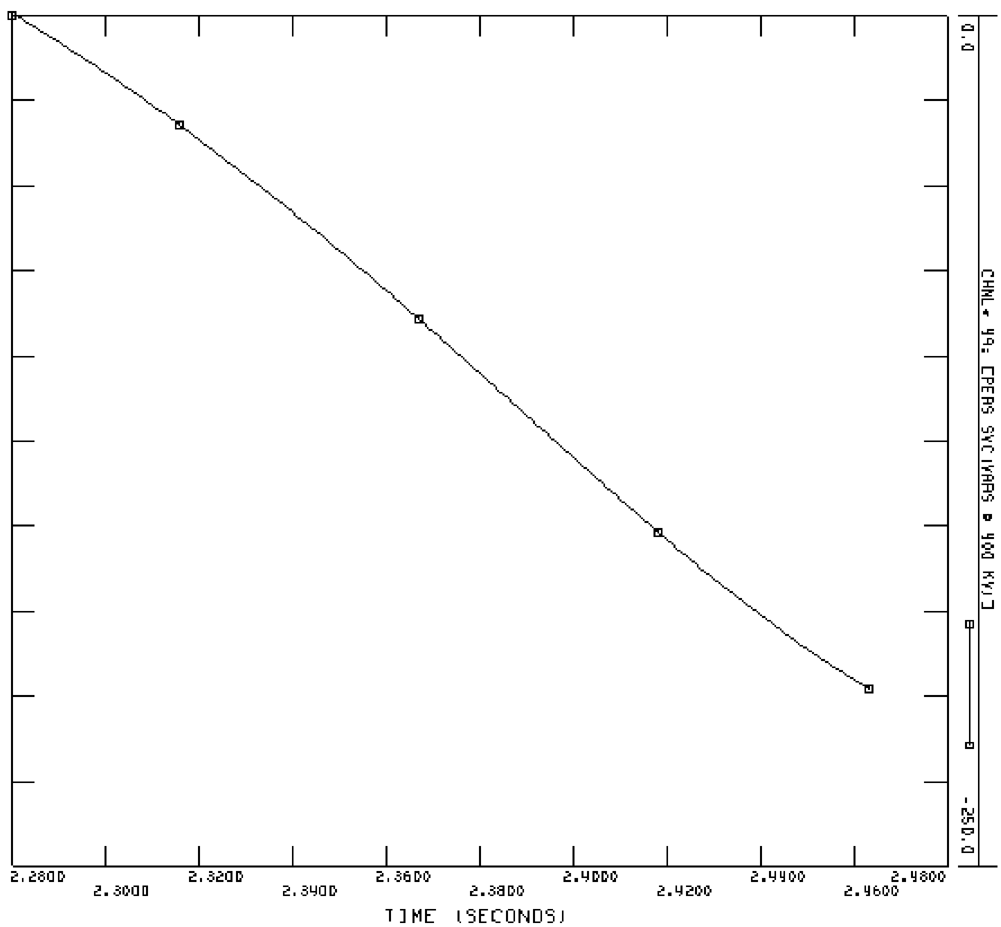

FIGURE 4.7 Response time of the TCR

4.1.3 Protection schemes that could operate due to fluctuations in voltage

Figure 4.8 shows the P531 recording of the power angle that developed between Mpumalanga and the Western Cape during the 7th June 1996 incident. During this incident, the Mpumalanga generation pool and the Western Cape generation pool operated asynchronously to the extent pole slipping occurred.

The slip frequency of this incident is 1.72 Hz (figure 4.8). Such high slip frequencies are not uncommon - 1 Hz was the slip frequency of an out-of-step event that occurred in the Japan network [33, p941].

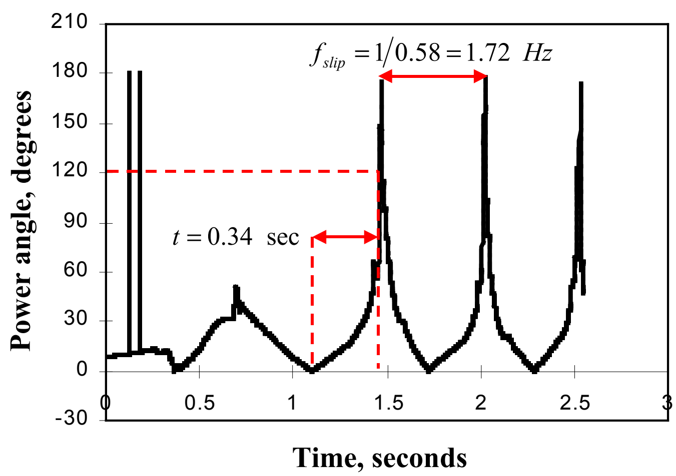

FIGURE 4.8 Digital Fault Recorder data of the Hydra-Droërivier power angle

A slip frequency of 1.72 Hz means it takes 0.58 seconds to complete the slip cycle.

Presently all the out-of-step relays installed in the Eskom network are set to “Trip-On-the-Way-Out” (TOWO).

TOWO issues the trip signal approximately when $\delta = 240^\circ$. Hence, for the incident shown in figure 4.8 the network is severed at approximately 0.42 seconds into the out-of-step event.

To clarify the 0.42 seconds, we note it takes approximately 0.34 seconds to move from steady state ($\delta = 0.0^\circ$) to $\delta = 240^\circ$ (operation beyond 180°, i.e. $180 + \Delta\delta$, is represented in figure 4.8 using $180 - \Delta\delta$ - hence 240° is shown as $180^\circ - 60^\circ$); the majority of line breakers installed at 400 kV take 80 milliseconds to open.

Therefore, the network is severed at approximately $0.42 = (0.34 + 0.08)$ seconds into the out-of-step event.

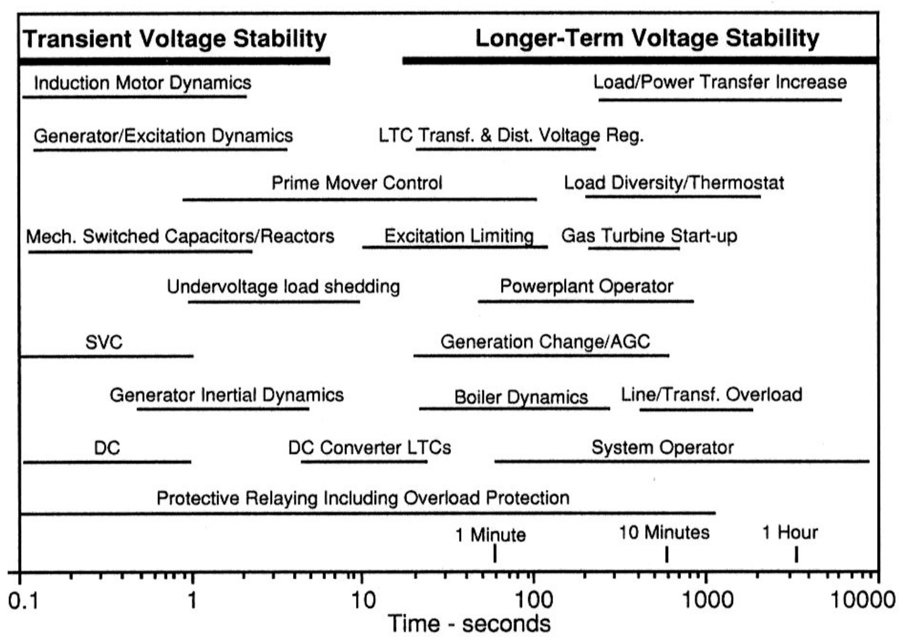

FIGURE 4.9 The time it takes different power equipment to react to a change in the voltage [34, p19]

Not all power plant act within the first 0.42 seconds of a network event. Figure 4.9 shows protective relaying (including overload protection) and mechanically switched capacitors and reactors could operate at or before 0.42 seconds into the out-of-step event.

The protective relaying schemes that could operate due to the voltage excursions occurring when slipping poles are the feeder distance protection, over- and undervoltage protection and overcurrent protection (figure 4.9).

4.1.3.1 Feeder distance protection

The possible effect slipping poles has on feeder distance protection is discussed in Chapter 2, section 2.7.

This dissertation assumes all the distance relays protecting the feeders that make up the Mpumalanga-to-Western-Cape tie line are equipped with out-of-step blocking schemes. Hence, it is reasonable to assume the feeder distance protection would not trip when the network is slipping poles.

4.1.3.2 Steady state overvoltage protection

At power angles close to $\delta = 360^{\circ}$ the line I^2X losses reduce significantly. This could lead to a situation where the VARs the shunt capacitors and the VARs the line charging inject into the network become excessive. Overvoltages will then occur. Hence, overvoltage protection could operate during the out-of-step event.

To explain the affect overvoltages could have, we consider the section of the Eskom network that operates at 400 kV.

We define the nominal voltage, U_{nom}, and the maximum voltage, $U_{\max} = 1.05 \times U_{nom}$. For the section of network considered, $U_{nom} = 400$ kV and $U_{\max} = 1.05 \times U_{nom} = 420$ kV.

The plant affected by permanent overvoltages are transformers, reactors, capacitors and arrestors [35, p33].

The voltage withstand capability is inversely proportional to time. Every equipment type has its own voltage withstand characteristic.

To protect transformers, Eskom specifies a withstand of 120% of $U_{\max}$ for 3 seconds [35, p32]. 120% of $U_{\max}$ for a 400 kV network is 504 kV.

To protect reactors, Eskom specifies a withstand of 120% of $U_{\max}$ for 3 seconds [35, p32]. Irrespective of the specification, no overvoltage protection is provided on reactors. The reason is the tripping of a reactor increases the network voltage. Reactors can fault due to overvoltage [35, p150]

To protect capacitors, Eskom specifies a withstand of 110% of U_{nom} for 0.2 seconds [35, p32].

To protect the transmission feeders, overvoltage relays could be installed. When installed these relays are set to 120% of U_{nom} for 2 seconds [35, p32].

Arrestors are designed to clamp the network voltage at 140% of U_{nom}. The duration arrestors can clamp the voltage is only a few seconds. For a longer duration or for shorter duration, but in quick succession, the arrestor will overheat and create a network fault [35, p150].

For the case where Mpumalanga and the Western Cape are slipping poles the network voltage will be high when the power angle between Mpumalanga and the Western Cape is approximately 0°. Hence, the overvoltages occurring during the out-of-step event are present for only a small portion of the slip cycle.

The expected period of the slip cycle is approximately 0.58 seconds (figure 4.8). In addition, the network is severed during the first slip cycle. Hence, the duration of the overvoltages will be much less than 0.58 seconds.

Not all the equipment mentioned trip within 0.58 seconds of an overvoltage - only capacitors and surge arrestors could.

With regard to the overvoltage protection of the shunt capacitors, we note the overvoltage protection of capacitors can be set to operate within 0.58 seconds - normal setting Eskom applies is 110% of nominal voltage for 0,2 seconds. Increasing the time setting to 3 seconds can be considered [35, p150].

With regard to surge arrestors, we note consecutive overvoltages can make surge arrestors fault within 0.58 seconds.

In Eskom, no record exists of shunt capacitors that tripped or surge arrestors that faulted during an out-of-step event.

Therefore, this dissertation does not model the operation of overvoltage protection on shunt capacitors and does not model the effect overvoltages have on surge arrestors.

4.1.3.3 Transient overvoltage protection

Transient overvoltages result from the opening of breakers, energising of an open-ended line, breaker/isolators re-striking during the opening of a capacitive load, interruption of current and lightning discharges [35, p14].

Except for lightning, the time frames of the above listed events are of the order of milliseconds. The time frame of the transient overvoltages due to lightning discharges is of the order of microseconds [35, p14].

Figure 4.10 shows that the time period of oscillations in power angle, δ, range from 0.1 seconds up to 10.0 seconds. These values are based on the time period of the slowest oscillation (10.0 seconds or 0.1 Hz) possible in networks that are dynamically stable and the time period of the fastest oscillation (0.5 seconds or 2.0 Hz) possible in networks that are dynamically stable [1, p818]. For transiently unstable networks the time period of the oscillation decreases. The smallest time period is 0.1 seconds (i.e. 10.0 Hz).

Hence, the time frames of transient overvoltages are much smaller than the time frame of an out-of-step event. In addition, the above listed transients are not due to the power angle changing. Therefore, this dissertation assumes no transient overvoltages are present during the out-of-step event.

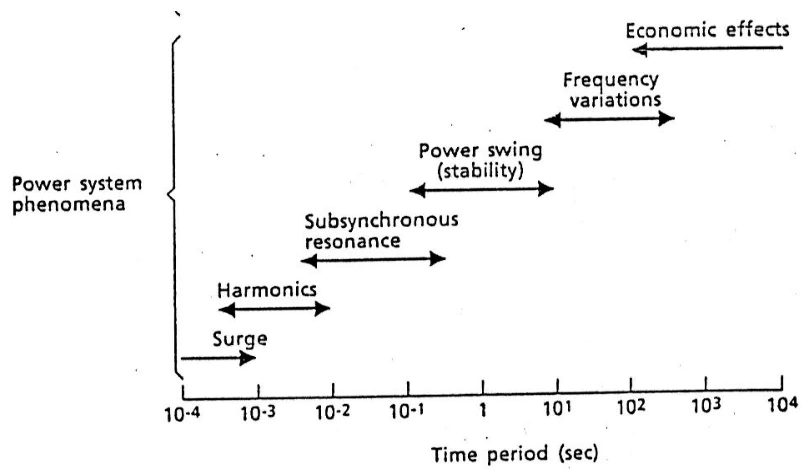

FIGURE 4.10 Network phenomena and their time frames [36, p962]

4.1.3.4 Losing customer plant

When the power angle, δ, between the generators slipping poles increases the line current increases. This large line current makes the busbar voltage located well within the network drop. When the power angle closes up the voltage profile recovers.

For the case where Mpumanaga and the Western Cape are slipping poles it will take approximately 0.58 seconds to complete the above sag and recovery of the voltage (figure 4.8). The depth of the sag in voltage increases the closer the busbar is situated to the electrical centre.

Table 4.4 shows that the sag and recovery in voltage could make customers lose load.

The reasons for the load loss are: Variable speed drives could trip due to operation of their undervoltage protection or overcurrent protection; motor contactors drop out due to a lack of voltage to the coils; control circuits malfunction and trip the process; motors stall when the majority of the motors attempt to accelerate on a weak network after the sag and physical damage or failure of power electronic devices due to high currents or due to fuses operating [37, p39].

Table 4.4 Definition of the NRS-048 Dip Chart [37, p40]

DIP CATEGORY	PARAMETER VALUE		BASIS FOR DEFINITION
Y	Duration	20ms – 3 sec	Dip definition (20ms to 3 s)
	Depth	20%	Minimum plant compatibility requirement
X	Duration	20ms – 150ms	Typical Zone 1 clearance (no pilot wire)
	Depth	20%-60%	Plant compatibility (drives trip > 20%) Caused by remote faults on the utility network
S	Duration	150ms–600ms	Typical Zone 2 and accelerated clearance
	Depth	20%-60%	Plant compatibility (drives trip > 20%) Caused by remote faults on the utility network
T	Duration	20ms – 600ms	Zone 1 and zone 2 clearance times
	Depth	60% - 100%	Plant compatibility (contactors trip > 60%)* Caused by close-up faults on the utility network
Z	Duration	600ms – 3s	Back-up and thermal protection clearance
	Depth	20% - 100%	Post-dip motor recovery without stalling

* Note: Defined at 60% rather than 50% as this ensures most of the motor contactors have dropped out and motor stability, i.e. post-dip re-acceleration, is not a problem.

With regard to motors, we note the electromagnetic held contactors of industrial motors drop open at voltages in the range of 0.55 to 0.75 p.u. The drop out time is in the order of a few cycles. Small motors on refrigerators and air conditioners have only thermal overload protection, which typically trip in about 10 to 30 seconds [1, p275].

Managing the effect of voltage dips on the plant is a joint effort between the customer and the utility. The respective responsibilities are: Utilities should manage protection clearance times (e.g. X-type dips allowed exceeds S-type dips allowed); utilities should place emphasis on the number of faults occurring close to a particular customer (e.g. sum of X-type and S-type dips is less than T-type dips) and by specifying the dip sensitivity of their process equipment customers can ensure the number of utility fault events affecting their plant is limited [37, p39].

Commercially available dip mitigation technologies are used to achieve the dip sensitivity the customer specifies.

Experience obtained from cases where the Eskom network was severed on the second or subsequent slip cycles (i.e. out-of-step relays failed to operate) showed dip-sensitive customers lose load on the second and maybe the third slip cycle [11, p36]. This shows the dip mitigation technologies the customers installed safeguarded their plant against the first sag and recovery in voltage.

This dissertation assumes out-of-step tripping is issued before the first slip cycle is completed. The load loss will then be a minimum.

Based on the above this dissertation does not model any loss of load due to the voltage dips that occur when slipping poles.

In addition, we note any attempt to predict the loss of load during an out-of-step event is a futile exercise. The reason is information regarding the composition of the customer plant (i.e. percentage of load comprising variable speed drives, the percentage of load with contactors, the dip sensitivity the customer specified for his plant, etc.) is not easily obtained.

4.1.4 Power plant that could be lost due to over-current

When $\delta = 180^\circ$ the voltage at the electrical centre is zero and the network behaves as if a three phase fault is present at the electrical centre. Hence, the protection devices installed on the series capacitors situated in the Mpumalanga-to-Western-Cape tie line could operate when the voltage at the electrical centre is zero.

To clarify, we note series capacitors are normally subjected to a voltage only a few percent of their rated voltage. When the line is short-circuited by a fault beyond the capacitor, e.g. when the electrical centre is located close to the capacitor bank, a voltage of the order of the line voltage appears across the series capacitors [1, p635].

To protect the series capacitors against such high voltages, the design of the series capacitors makes provision for bypassing the capacitor during faults and reinsertion after fault clearance. Traditionally, bypassing was provoked by a spark gap across the bank or each module of the bank. The present trend is to use non-linear zinc oxide arrestors which have the advantage that reinsertion is essentially instantaneous [1, p635].

All of the series capacitor banks installed in the Eskom network are equipped with a spark gap.

When the electrical centre is electrically close to the series capacitor bank the line current passing through the series capacitor is the capacitor bank's three phase fault current. Hence, flashover of the spark gap when slipping poles is possible.

Only certain post-contingency network topologies will result in the electrical centre being electrically close to the cap banks installed in the mentioned tie-line. Therefore, the probability of having series capacitors flashing over when slipping poles is very small.

Record of a series capacitor bank flashing over when slipping poles exists for only one of the incidents where the Eskom network operated asynchronously to the extent slipping of poles occurred [10, p3].

Due to this low probability this dissertation does not model the flashing over of series capacitor banks.

4.2 IMPROVED TWO GENERATOR MODEL ACCURACY ADEQUITE

This section shows that the improved two generator model can be used to illustrate the affect shunts have on the impedance locus the swing traces.

4.2.1 Inaccuracies due to the modelling used

The improved two generator model uses the constant voltage behind transient reactance generator model and keeps the external network impedance constant.

To show that the internal voltage of the generator can be regarded as constant, we note that the generator transient voltage stays approximately constant during the first slip cycle (Appendix H). Eskom applies out-of-step tripping during the first slip cycle. Hence, it is reasonable to use a constant voltage generator model.

Therefore, the modelling inaccuracies associated with the improved two generator model will be due to inaccurate modelling of the generator reactance and/or the external network impedance.

With regard to the generator reactance, we note the accuracy with which a single generator reactance, $x^{'}$, represents armature reaction depends on the angle the generator current forms with the q-axis (Appendix H).

The detailed network model considers magnetic saliency. The improved two generator model does not consider magnetic saliency. This makes $\left|\boldsymbol{E}^{'}_{MPU}\right|$ and $\left|\boldsymbol{E}^{'}_{KBG}\right|$ to differ between the former and latter network models (Appendix D). Figure 4.13 and figure 4.14 show the error in $\left|\boldsymbol{E}^{'}\right|$ does not make the impedance locus the improved two generator model traces differ greatly from the impedance locus the detailed network model traces.

With regard to the external network impedance, we note the two generator model keeps the external network impedance constant. The detailed network model uses the same modelling except the SVCs are modelled using model CSVGN1. Figure 4.13 and figure 4.14 show the simple shunt SVC model that the two generator model uses does not make the impedance locus the improved two generator model traces differ greatly from the impedance locus the detailed network model traces.

4.2.2 The swing locus the improved two generator model traces

4.2.2.1 The steady state networks

The tie line and the generation pools on both sides of the tie line make up the basic steady state network.

The load flow of the tie line of the improved two generator model matches the load flow of the tie line of the detailed network model (Chapter 3, section 3.5.6).

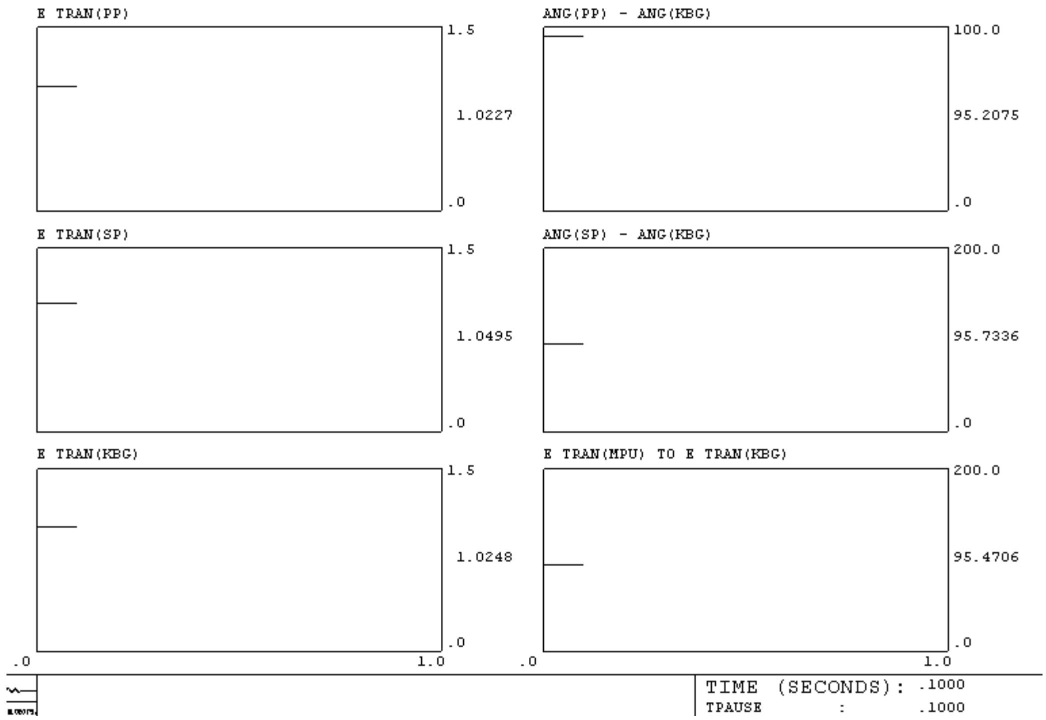

FIGURE 4.11 The voltage behind transient reactance and the angle it has when the detailed network model is in steady state

The remainder of this section shows that the operating point of the generators situated in the improved two generator model match the operating point of the same generators situated in the detailed network model.

To show that the operating point of the above generators is the same, the voltage behind transient reactance is compared. To ensure that the effect magnetic saliency has on $\left|\boldsymbol{E}^{'}\right|$ (Appendix D) and thus on $\delta_{MPU} - \delta_{KBG}$ does not introduce errors when comparing $\boldsymbol{E}^{'}$, the generators in the detailed network model are modelled using the constant voltage behind transient reactance generator model.

Figure 4.11 shows the first 100 milliseconds of a steady state simulation run on the detailed network model. This study obtains the magnitude, $\left|\boldsymbol{E}^{'}\right|$, of the voltage behind transient reactance and the angle $\boldsymbol{E}^{'}$ forms with the synchronously rotating reference.

Figure 4.12 shows the first 100 milliseconds of a steady state simulation run conducted on the improved two generator model. This study obtains the magnitude, $\left|\boldsymbol{E}'\right|$, of the voltage behind transient reactance and the angle $\boldsymbol{E}'$ forms with the synchronously rotating reference.

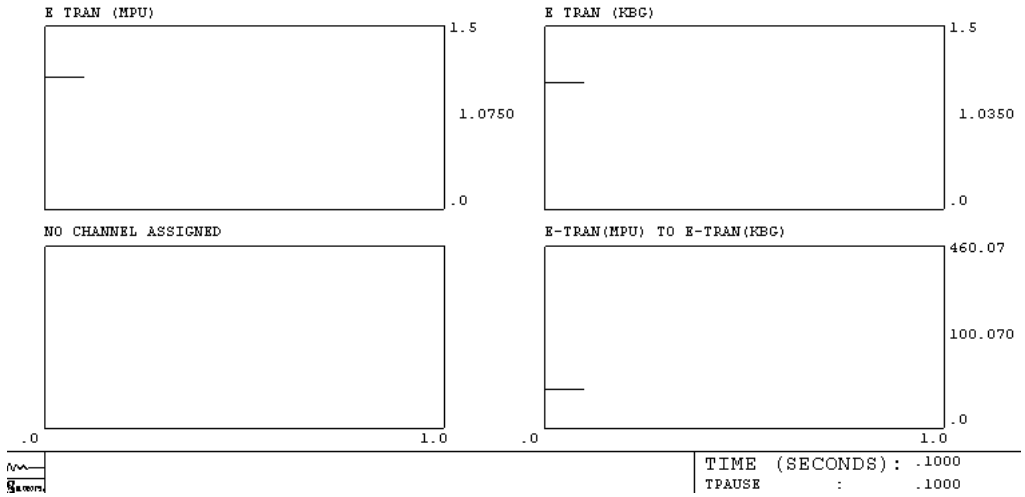

FIGURE 4.12 The voltage behind transient reactance and the angle it has when the improved two generator model is in steady state

The power angle, δ, that develops between the voltage behind transient reactance of the Mpumalanga, $\boldsymbol{E}'_{MPU}$, and the Koeberg, $\boldsymbol{E}'_{KBG}$, generators can be computed using (Appendix A, equation A.1 and equation A.5):

$$\begin{aligned} \delta &= \delta_{MPU} - \delta_{KBG} \\ &= \frac{(\delta_{PP} + \delta_{SP})}{2} - \delta_{KBG} \end{aligned} \tag{4.4}$$

In the detailed network model, $\delta = 95.47$ degrees (figure 4.11) and in the improved two generator model, $\delta = 100.07$ degrees (figure 4.12).

$\left|E'_{MPU}\right|$ can be computed using (similar to the computation of δ_{MPU}):

$$\left|E'_{MPU}\right| = \frac{\left|E'_{PP}\right| + \left|E'_{SP}\right|}{2} \tag{4.5-a}$$

For the detailed network model (figure 4.11) we have:

$$\left|E'_{MPU}\right| = \frac{1.0227 + 1.0495}{2}$$

$$= 1.036 \text{ p.u.} \tag{4.5-b}$$

$$\left|E'_{KBG}\right| = 1.0248 \text{ p.u.} \tag{4.5-c}$$

For the improved two generator model $\left|E'_{MPU}\right| = 1.075$ p.u. and $\left|E'_{KBG}\right| = 1.035$ p.u. (figure 4.12).

Table 4.5 shows that the value of δ in the improved two generator model matches the value in the detailed network model.

Table 4.5 Comparing the improved two generator model and the detailed network model with regard to power angle

PARAMETER	VALUE OBTAINED IN IMPROVED TWO GENERATOR MODEL [Degrees] A	VALUE OBTAINED IN DETAILED NETWORK MODEL [Degrees] B	ACCURACY [%] (A/B)×100
$\delta_{MPU} - \delta_{KBG}$	100.07	95.47	104.82

Table 4.6 shows that the magnitudes $\left|E'_{MPU}\right|$ and $\left|E'_{KBG}\right|$ in the improved two generator model match the magnitudes in the detailed network model.

Table 4.6 Comparing the improved two generator model and detailed network model with regard to the voltage behind transient reactance

PARAMETER	VALUE OBTAINED IN IMPROVED TWO GENERATOR MODEL [p.u.] A	VALUE OBTAINED IN DETAILED NETWORK MODEL [p.u.] B	ACCURACY [%] (A/B)×100
$\lvert E'_{MPU} \rvert$	1.075	1.036	103.76
$\lvert E'_{KBG} \rvert$	1.035	1.025	100.98

4.2.2.2 The transiently unstable networks

To show the improved two generator model does not over or under emphasise the affect shunts have, the impedance locus the model traces should match the impedance locus the detailed network model traces.

The generators situated in the improved two generator model are modelled using the constant voltage behind transient reactance model. The load is constant impedance and constant admittance shunts are used to model the SVCs.

The generators situated in the detailed network model are modelled using model GENROU. The load is constant impedance and the SVCs are modelled using model CSVGN1.

Both the former and latter models are made transiently unstable by weakening the network as is discussed in Chapter 3, section 3.3

To show that shunts could make the impedance locus differ greatly from the locus when the shunts are omitted, the impedance locus is constructed for the case where the out-of-step relay is located at Hydra and looks towards Mpumalanga (Chapter 5, section 5.1.1 and section 5.1.2).

To show that the swing behaves classically when observed from a location that is the electrical centre, the impedance locus is constructed for the case where the out-of-step relay is located at Hydra and looks towards Koeberg (Chapter 5, section 5.1.5).

To show that the above two illustrations are realistic, the remainder of this section shows that the two generator model traces a swing locus that matches the swing locus the detailed network model traces.

The interval $\delta \in \left[120^\circ;240^\circ\right]$ is the range of power angles for which the swing loci compared should match (Chapter 2, section 2.11).

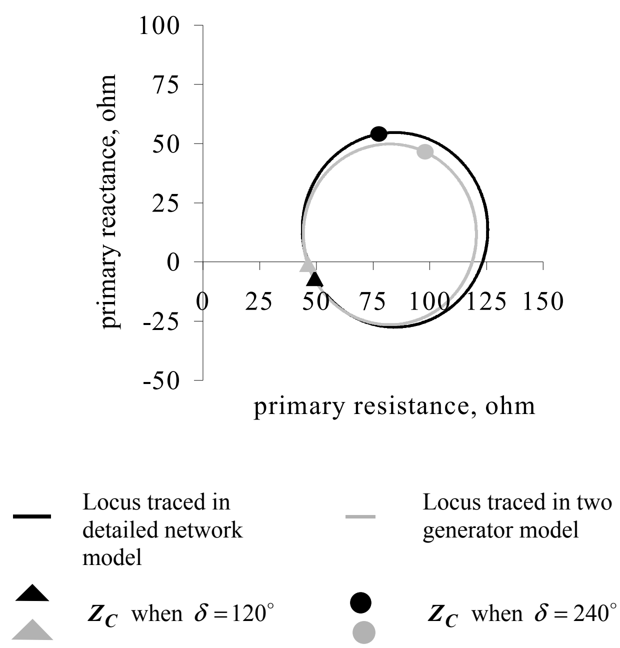

FIGURE 4.13 Comparing the impedance locus that the improved two generator model traces with the impedance locus the detailed network model traces (out-of-step relay is located at Hydra looking towards Mpumalanga)

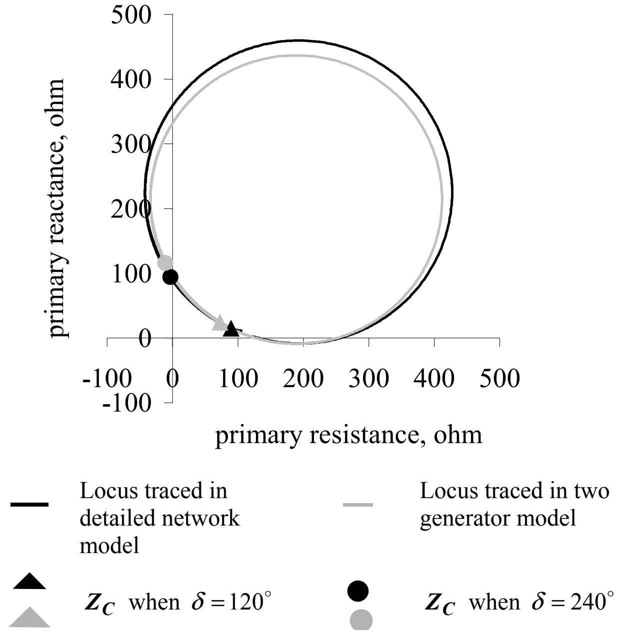

FIGURE 4.14 Comparing the impedance locus that the improved two generator model traces with the impedance locus the detailed network model traces (out-of-step relay is located at Hydra looking towards Koeberg)

Figure 4.13 and figure 4.14 show that the locus the improved two generator model traces matches the locus the detailed network model traces when compared for the power angles $\delta \in \left[120^\circ;240^\circ\right]$.

Hence, the improved two generator model traces a swing locus that matches the real swing locus (i.e. swing locus detailed network model traces). Therefore, the improved two generator model can be used to demonstrate the affect shunts have on the swing locus.

The resistive and reactive components of the swing loci shown in figure 4.13 and figure 4.14 are computed using (Chapter 2, equation 2.4):

$$\boldsymbol{Z_C} = \frac{P_C V_C^2}{P_C^2 + Q_C^2} + \boldsymbol{j}\,\frac{Q_C V_C^2}{P_C^2 + Q_C^2} \tag{4.6}$$

$V_C = |\boldsymbol{V_C}|$ is the magnitude of the voltage at the relay location (i.e. Point C); Q_C is the reactive power flowing at Point C and P_C is the active power flowing at Point C.

The procedure followed to mark the network condition $\delta = 120^\circ$ and $\delta = 240^\circ$ on the swing loci shown is discussed in Appendix I.

4.3 EFFECT INDUCTION MOTORS HAVE ON THE SWING LOCUS

This section shows that the swing locus the improved two generator model traces is not the swing locus that real networks trace.

The above is illustrated by comparing the impedance locus the improved two generator model traces with the impedance locus the detailed network model traces when the load situated in the detailed network model includes large and small induction motors.

Figure 4.15 and figure 4.16 show the impedance locus the detailed network model traces when model CLOAD is used to model the load south of Tutuka, Atlas and Grootvlei. The load north of Tutuka, Atlas and Grootvlei is modelled using a ZIP model. The real part of the ZIP model is constant current and the imaginary part is constant impedance.

Table 4.2 and table 4.3 list the parameters CLOAD uses.

Figure 4.15 and figure 4.16 show that the swing locus has two phases. During the initial stage, i.e. first phase, the swing locus is approximately a straight line. The impedance locus traced from Point A to Point B (figure 4.15) is the initial stage.

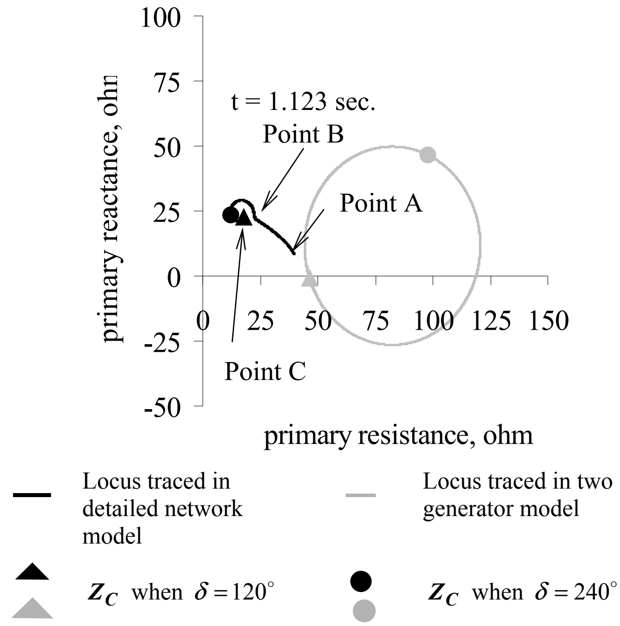

FIGURE 4.15 Impedance locus the detailed network model traces (out-of-step relay is located at Hydra looking towards Mpumalanga). The impedance locus the improved two generator model traces is also shown - load is constant impedance

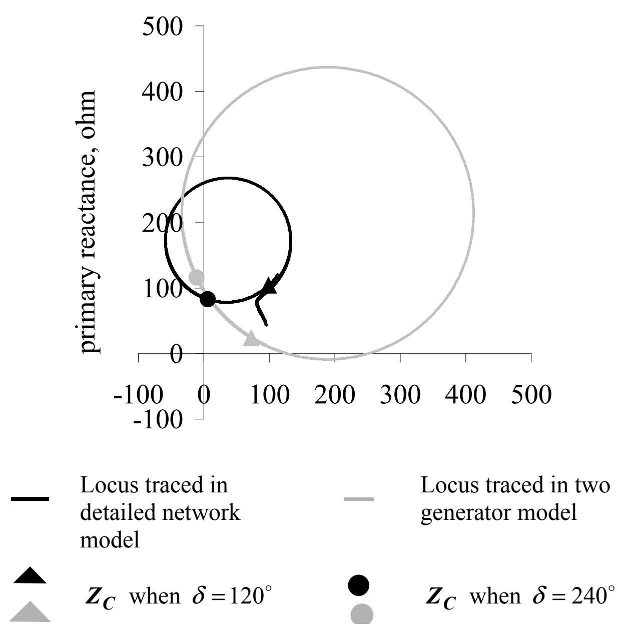

FIGURE 4.16 Impedance locus the detailed network model traces (out-of-step relay is located at Hydra looking towards Koeberg). The impedance locus the improved two generator model traces is also shown – load is constant impedance

After a while, the swing traces a circular impedance locus. This is the second stage. For the swing locus shown in figure 4.15, the second stage is the locus traced from Point B to Point C.

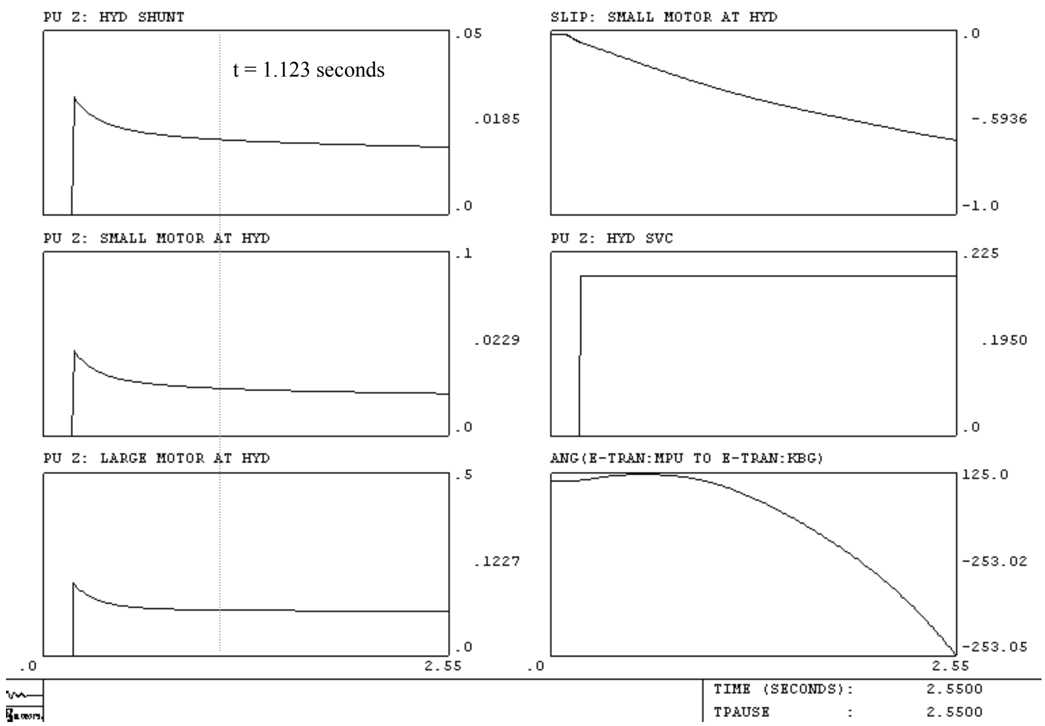

FIGURE 4.17 Impedance magnitude and slip traced for the aggregated large and small induction motors at Hydra. The impedance of the equivalent shunt at Hydra is also traced

The first phase is due to the motor slip changing. This makes the induction motor impedance change. The motor impedance decreases up to where the impedance becomes insensitive to slip. In figure 4.17 this happens when $t = 1.1.23$ seconds. In figure 4.15 time $t = 1.123$ seconds is marked "Point B".

For the remainder of the slip cycle, i.e. beyond $t = 1.123$ seconds, the motor impedance settles. This makes the swing trace a circular impedance locus.

When the load that is situated in the detailed network model includes large and small induction motors, the swing locus the improved two generator model traces is greatly different from the swing locus the detailed network model traces (figure 4.15 and figure 4.16).

Hence, the improved two generator model should only be used to understand the results obtained with more complex networks.